662 *Macromolecules* **2010**, *43*, 662–670
DOI: 10.1021/ma902109r

Macromolecules
ARTICLE

Role of Aniline Oligomeric Nanosheets in the Formation of Polyaniline Nanotubes

Zoran D. Zujovic,*,† Cosmin Laslau,† Graham A. Bowmaker,† Paul A. Kilmartin,† Amy L. Webber,‡ Steven P. Brown,‡ and Jadranka Travas-Sejdic*,†,§

†*Polymer Electronics Research Centre, Department of Chemistry, University of Auckland, Private Bag 92019, Auckland, New Zealand,* ‡*Department of Physics, University of Warwick, Coventry CV4 7AL, United Kingdom, and* §*MacDiarmid Institute for Advanced Materials and Nanotechnology, New Zealand*

Received September 22, 2009; Revised Manuscript Received November 18, 2009

ABSTRACT: We report the phenomenon of nanosheet rolling during typical aqueous polymerization and study its implications for the self-assembly of polyaniline nanotubes. Specifically, this is done through a detailed morphological and structural characterization of products obtained after 20 min, 1 h in falling pH experiments, and after 20 h at constant pH 2.5 during the oxidative polymerization of aniline with ammonium persulfate in the presence of alanine. The chemical structure has been investigated by FTIR, UV−vis, solid-state ^{13}C and ^{15}N NMR, liquid NMR, and XRD, whereas the morphology was imaged using scanning electron microscopy (SEM) and transmission electron microscopy (TEM). The presence of self-assembled nanoflakes with different thicknesses ranging from tens to hundreds of nanometers is confirmed through SEM. TEM revealed the presence of very thin layers: nanosheets with sharp and well-defined edges. The presence of hydrogen bonds is confirmed by FTIR and is consistent with XRD results. The stacking of nanosheets and the formation of thicker flakes based on $\pi-\pi$ electron interactions have been proposed on the basis of XRD experiments, where self-assembled layers made of cross-linked oxidized aniline structures stack on each other and are stabilized by hydrogen bonds and $\pi-\pi$ interactions. In this way, hydrophobic cross-linked oligomers (formed at the beginning of the synthesis at higher pH) minimize their surface energy, self-assembling into well-ordered macromolecular structures. On the basis of the SEM and TEM images and the information obtained from other analytical techniques applied here, the presence of PANI nanotubes formed in the reaction carried out at constant pH of 2.5 is confirmed. The role of the nanosheets in the formation of nanotubes is proposed.

Introduction

The conducting polymer polyaniline (PANI) is typically produced in the oxidative polymerization of aniline using a strong oxidizing agent such as ammonium persulfate (APS) in a strong acidic solution such as 1 M HCl.[1,2] Synthesized in this way, PANI possesses a granular morphology that is characterized by irregular agglomerates and high conductivity. However, under certain conditions, PANI can form supramolecular ordered nanostructures (nanotubes, nanorods, nanofibers, and nanospheres), the formation and structural characteristics of which have been extensively studied and reported.[3−25] Interest in this area stems from the applications that these nanostructures might find in sophisticated micro- and nanoelectronic circuit components with advanced functions.[15,26,27] The understanding of the formation mechanism and control of the size and functions of PANI nanostructrures has become important for their production and application in nanodevices. In recent years, many reports have focused on the self-assembly of PANI nanostructures, especially nanotubes and nanofibers.[20−25,28−31] However, the detailed chemical mechanism of their self-assembly has yet to be fully understood.

In previous reports[6,19,20,32] on self-assembled PANI nanotubes, we investigated their structural characteristics and conditions for formation. A typical synthesis starts at a pH of ∼7.5, and during the course of the 20 h reaction, the pH drops to ∼1.0. Interestingly, morphologically different products are formed during the synthesis as a function of pH.[19,20,32] After 1 h from the beginning of the reaction, the sample showed nanoflake morphology.[19,20] The morphology remained essentially the same up to 3 h, whereupon fibrilar structures were noticed. At the end of reaction (after 20 h), in addition to the flakes that were present, predominantly fibrous morphologies such as nanofibers and nanotubes were observed.[19,20] Therefore, the final product synthesized through the "falling pH" reaction is not morphologically homogeneous, a fact that should be taken into account during structural investigations. It has been pointed out that the complex formation of self-assembled PANI nanotubes depends on molecular interactions such as hydrogen bonding, van der Waals forces, and $\pi-\pi$ stacking.[6−25] These forces are also likely to be operational throughout the early stages of the synthesis, when the nanoflake morphology is predominant. We propose that interactions and reaction mechanisms in an early stage can be more easily and accurately identified rather than in later stages, when the sample becomes morphologically (and likely structurally) heterogeneous. Specifically, we hypothesize that there are two key stages underpinning the formation mechanism. The first one is when nanosheets, formed in the first stage of oxidative polymerization at higher pH, tend to decrease the surface energy either through stacking, when relatively thick (∼30−100 nm) nanoflakes are formed,[20] or by rolling or curling, when oligomeric nanotubes are formed. This mechanism is very similar to the formation of a number of tubular inorganic materials (such as those made from Fe_3O_4, BN, V_2O_5, WS_2,

*Corresponding authors. E-mail: z.zujovic@auckland.ac.nz (Z.D. Z.); j.travas-sejdic@auckland.ac.nz (J.T.-S.).

 Published on Web 12/22/2009

and $NiCl_2$) from 2-D layered precursors at elevated temperatures, based on a "rolling-up" mechanism.[33] The second stage takes place later in the reaction at lower pH, when polyaniline either polymerizes from the oligomeric nanotube walls or simply covers up the walls of smooth nanotubes with grains, making these walls thicker and giving the final form of the PANI nanotubes or nanorods, as has been shown in our previous work.[34] Therefore, our focus in this article will be mainly toward the elucidation of the structure of 2-D nanosheets and their role in the formation of nanoflakes or oligomeric nanotubes.

To tackle the important problem of the chemical nature and the role of initial structures and the corresponding molecular interactions during the formation of PANI nanotubes, the following experiments have been performed: (a) A falling pH experiment has been carried out at ambient temperature. A small sample of the product 20 min after the beginning of the reaction was taken and extensively diluted with water to slow down the reaction. We avoided filtration or centrifugation, as this may disturb the delicate structures formed in the early stage of the reaction. Instead the sample was left to settle naturally, and after 5 days, a sample of the solid phase was taken out for SEM and TEM. (b) A pH stat experiment,[32] in which pH was kept constant at 2.5 throughout most of the reaction, was performed. The pH region at ~2.5 was chosen because this may be where the PANI nanotubes form in highest yield.[32] In this way, the "high pH" and the "low pH" parts of the reaction are avoided when it is considered that most of the probably hydrophobic[35] nanoflakes and granular polyaniline are formed during the falling pH reaction. The formation and the structural characteristics of these products are discussed on the basis of SEM, TEM, FTIR, UV−vis, XRD, and solid-state NMR data.

Experimental Section

Materials. ^{15}N labeled aniline and ammonium persulfate ($(NH_4)_2S_2O_8$, APS) were obtained from Aldrich. The amino acid alanine was purchased from Sigma. They were used as received without further treatment.

Synthesis. *"Falling pH" Experiments*. Aniline (0.182 mL, 0.1859 g, 2.0 mmol) and alanine (0.0356 g, 0.4 mmol) were dissolved in 10 mL of Milli-Q water and, separately, APS (0.464 g, 2.0 mmol) was dissolved in 5 mL of Milli-Q water. The solutions were precooled at 5 °C for 30 min, after which they were mixed to give final concentrations of aniline = 0.133 mol L^{-1}, alanine = 0.027 mol L^{-1}, and APS = 0.136 mol L^{-1}. The reaction beaker was placed in a water bath at 5 °C. The mixture was not stirred during the reaction. The precipitate after 1 h of the reaction was collected and washed with water and dried in vacuum at room temperature for 24 h, giving a light brown powder ("falling pH 1 h" sample). A separate experiment was performed to obtain the product after 20 min of the reaction, where the reaction conditions were the same as those above, except that the reaction was performed at room temperature. The reaction is faster, and it was easier to control the timing of sampling. The reaction solution (200 μL) was taken and extensively diluted with water to slow down the reaction. To not disturb the early formed structures by filtration or centrifugation, the sample was left to naturally settle, and after 5 days, the solid sample was isolated for SEM and TEM experiments ("falling pH 20 min" sample). A third experiment, under the same conditions, was done to record the pH evolution during the reaction by a pH-monitoring apparatus consisting of a Metrohm 836 Titrando base, 804 Ti stand, stirrer, electrode, water bath, and software.[32]

pH Monitoring. The pH-monitoring apparatus consisted of a Metrohm 836 Titrando base, 804 Ti stand, stirrer, electrode, water bath, and software. The solution was stirred at 250 rpm, and the water bath was precooled at 5 °C. A detailed description of this apparatus is reported elsewhere.[32]

pH-Stat Experiments. pH-stat experiments were performed at constant pH 2.5, where sulfuric acid was quickly added at the very beginning of the reaction to reach pH 2.5,[32] followed by maintaining pH at 2.5 by the pH-monitoring apparatus described above. The other conditions of the reaction were the same as those above. In the first pH-stat experiment, 200 μL of the reaction solution was transferred to 10 mL of aqueous solution of pH 2.5 to both slow the reaction and ensure that the pH was maintained at ~pH 2.5. (The pH 2.5 aqueous solution was simply obtained by diluting the necessary amount of sulfuric acid into Milli-Q purified water, with pH monitored using the aforementioned Metrohm apparatus as the acid was added until pH 2.5 was reached.) The solution was then quickly taken for TEM analysis and imaged within 20 min ("pH 2.5 20 min" sample). The second pH-stat experiment was performed under the same conditions except that the reaction was allowed to run for 20 h, and the final product was filtered, washed with water, and vacuum-dried at room temperature for 24 h ("pH 2.5 20 h" sample).

Standard Synthesis of Polyaniline. Standard polyaniline was synthesized according to the procedure reported elsewhere.[36] The "pH 2.5 20 h" and standard polyaniline samples were dedoped with 15% NH_4OH.

UV−Visible Spectroscopy. For UV−vis spectroscopy, the samples were dissolved in *N*-methyl-2-pyrrolidinone, and the spectrum was recorded using a Shimadzu UV-1700 spectrophotometer.

FTIR Spectroscopy. FTIR analysis of the samples was performed using the Smart Orbit ATR single reflection accessory of the Thermo Electron Nicolet 8700 FTIR spectrometer, with a Germanium crystal. The spectra were ATR corrected using the OMNIC spectroscopic software program.

XRD Measurement. X-ray diffractograms were obtained using a Rigaku MiniFlex II diffractometer. The speed was 1°/min using Cu Kα X-rays, a 2θ range of 5−70°, and a step ize of 0.02°. The power setting was 30 kV and 15 mA.

SEM Characterization. The morphology of the product was investigated using a Philips XL30S field emission scanning electron microscope (SEM). The sample for SEM was mounted on aluminum studs using adhesive graphite tape and sputter-coated with platinum.

TEM Characterization. A JEOL TEM-2010 transmission electron microscope (TEM) was used. The TEM sample of the "falling pH 1 h" sample was dispersed in water by ultrasonication and then pipetted onto copper-coated grids.

Solid-State NMR. All solid-state NMR experiments were carried out on dry powder samples using a Bruker AVANCE 300 spectrometer operating at 300.13 MHz proton frequency. Basic spectra were obtained by using the standard CP MAS (cross-polarization magic angle spinning) technique. The experiments were carried out using a 7 mm Bruker spinning probe with zirconia rotors. The magic angle was adjusted by maximizing the sidebands of the ^{79}Br signal of a KBr sample.

^{13}C CP MAS NMR Spectroscopy. The proton 90° pulse duration was 4.2 μs, and the frequency of the continuous wave decoupling field was 62.5 kHz. The contact time was 1.5 ms. The spectral width was 40 kHz. The ^{13}C chemical shift scale is referenced to TMS. The samples were rotated at 7000 ± 1 Hz.

^{15}N CP MAS NMR Spectroscopy. The proton 90° pulse duration was 7.3 μs, and the frequency of the continuous wave decoupling was 43 kHz. The contact time was 1.5 ms. ^{15}N chemical shifts were referenced to the external solid $^{15}NH_4Cl$ (δ $^{15}NH_4^+$ = 17.4 corresponding to $^{15}NH_4NO3$ = 0).[37a] Note that the ^{15}N spectra in our previous paper[20] were referenced on account of using solution-state reference scheme from Martin et al.[37b] where the δ $^{15}NH_4Cl$ 6.7 corresponds to $^{15}NH_4NO_3$ = 0. However, the reported samples were solids; therefore, the corrected chemical shift δ_{corr} for ^{15}N spectra given in Zujovic et al.[20] δ, should be $\delta_{corr} = \delta + 10.7$. This accounts for the chemical shift difference between the solid and liquid standard samples of

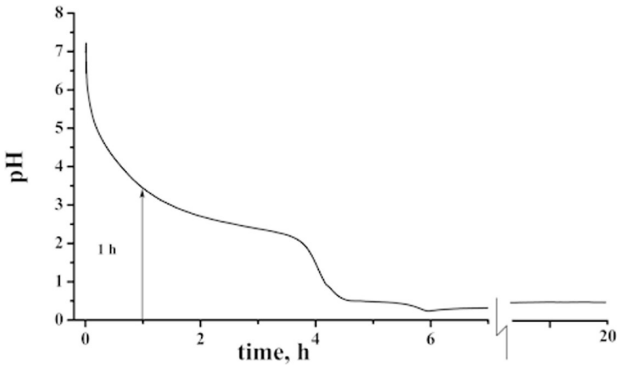

Figure 1. Evolution of pH during the chemical oxidation of aniline using APS as the oxidant and alanine.

$^{15}NH_4Cl$. The rotation frequency was 5000 ± 1 Hz for the polyaniline and 4500 ± 1 Hz for the "falling pH 1 h" sample.

Results and Discussion

Course of Oxidation. The complicated interplay between the formation of different oligomeric aniline products and polyaniline at different pH values during the "falling pH" reaction seems to be a key factor for the formation of self-assembled nanostructures. Information about the course of the aniline oxidation process itself and the resulting products obtained throughout the "falling pH" reaction was determined by monitoring the time dependence of the solution acidity. (See Figure 1.)[23,24] Aniline is a weak base (pK_a = 4.5 at 25 °C), and as such, at high pH, it exists in a neutral form, whereas at low pH, the anilinium cation form dominates. The "falling pH" reaction starts at a pH ~7.5, with an excess of neutral aniline molecules in the reaction mixture. Aniline is easily oxidized by APS to form dimers and oligomers, a process that releases protons and thus increases the aqueous solution acidity. As a result, nonconducting oligomers are produced at higher pH, composed of mixed para- and ortho-coupled aniline units.

As the pH decreases below 4.5, the equilibrium is shifted toward the formation of anilinium cations. These anilinium cations are significantly less oxidizable than the neutral form of aniline, which has a localized electron pair on the nitrogen atom. At pH values of 3 to 4, the intermediate, highly oxidized pernigraniline-like products (such as *N*-phenyl-1,4-benzoquinonediimine, B−*N*═Q═NH)[38] formed at the beginning of the reaction are not protonated in the reaction medium. Considering that the pernigraniline-like structures consist of conjugated double bonds, the unpaired electron positioned at the chain end becomes more delocalized along the backbone as the length of oligoaniline chains increases. Therefore, delocalization of the end-chain electron becomes more efficient, slowing down the polymerization in the oligomeric stage. Moreover, because of the occurrence of intermolecular cyclization, the ortho-coupled aniline units produced by oxidation of neutral aniline in an early stage (pH > 4.5) can be further transformed to *N*-phenylphenazines,[22−24] which have a high oxidation potential that can also suppress polymer growth. Consequently, the reaction slows down (the plateau between pH 2 and 3, Figure 1) but does not stop completely because of the oxidation of residual neutral aniline molecules.

The "falling pH 1 h" sample was taken at ~pH 3.5 (Figure 1) and was immediately centrifuged, washed, and dried to stop the polymerization reaction. According to the above arguments, we expect oxidized, para- and ortho-branched oligomeric aniline products to be present in this sample.

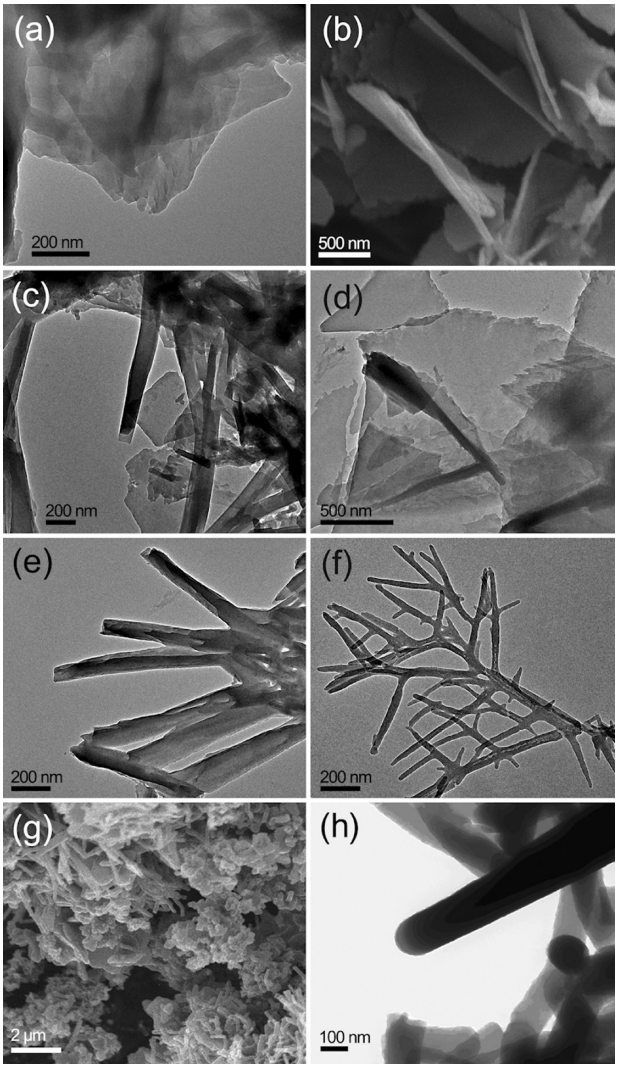

Figure 2. (a,c,d,e,f,h) TEM and (b,g) SEM micrographs of (a) the "falling pH 1 h" sample, (b−f) the "falling pH 20 min" sample at ambient temperature, and (g,h) the "pH 2.5 20 h" sample.

The slowing down period (the plateau around pH 2.5) is followed by the process of polymerization, that is, chain propagation at a pH below 2, when the polyaniline chains grow to produce the blue protonated pernigraniline form through the addition of anilinium cations in para-coupled positions. Also, the intermediate pernigraniline molecules become protonated and more prone to oxidation. This leads to the formation of high-molecular-weight polyaniline. The polymerization stops when the oxidant is depleted and when the protonated pernigraniline form is reduced by the residual aniline molecules, becoming green protonated emeraldine. (The last drop in the pH profile, a small shoulder around the 4.5 h mark, could be due to the transformation of pernigraniline to emeraldine.)[24]

SEM and TEM. The TEM micrograph of the ultrasonicated product obtained for the "falling pH 1 h" sample is shown in Figure 2a. After 1 h of reaction time, self-assembled rectangular, stacked nanosheets are observed,[19,20] probably partially exfoliated because of the ultrasonication.

According to previously reported results,[20] these should consist of oligomeric aniline products, with a mean molecular weight value of ~1300, corresponding to 10−15 monomer units. On the basis of the pH value at which this product was obtained, branched as well as linear structures would be

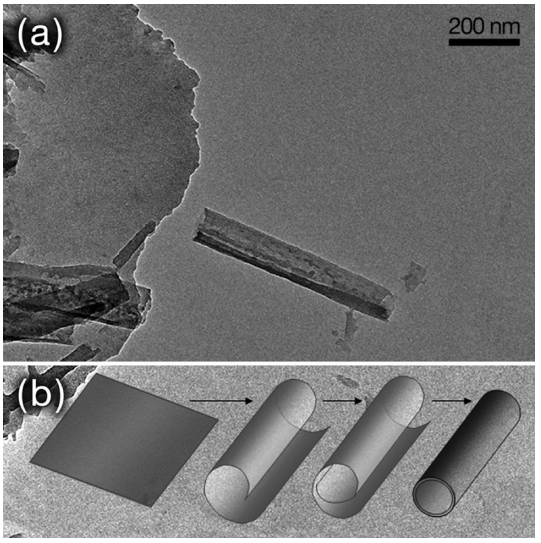

Figure 3. TEM micrograph of (a) the "falling pH 20 min" sample and (b) the corresponding scheme.

expected.[19] The thickness, estimated from the edges of the nanoflakes, lay in the range of approximately 30−100 nm.[20] It is evident that these structures do consist of a few nanometers thin layers. The molecular layers in these structures (nanosheets) could be linked by $\pi-\pi$ interactions or hydrogen bonding.[39,40] This is very similar to the formation mechanism of nanobelts obtained using *o*-phenylenediamine (OPD) and $FeCl_3$ aqueous solution.[41]

The nanosheets (besides the oligomeric nanofibrilar structures, Figure 2f) formed in the beginning of the reaction could serve as templates for the formation of 3-D structures very similar to the formation of a number of tubular inorganic materials based on a "rolling-up" mechanism.[33] The driving force for the rolling or curling behavior can be attributed to the minimizing of the surface free energy. The curling and its effects on the morphological characteristics of the products taken after 20 min of the reaction are shown in Figure 2b−e. The formation of irregular partially curled structures is shown in Figure 2b,d (SEM and TEM, respectively). These structures are more likely to be templates either for nanorods or PANI nanotubes with uneven inner bores. However, there are more regular tubular structures shown in Figure 2c, which could represent templates for more regular PANI nanotubes. Some of the structures shown in Figure 2e exhibit an incomplete tubular morphology. Besides nanosheet structures, there are also needlelike oligomeric structures (Figure 2f), which can serve as templates for the formation of nanorods, shown in Figure 2h. The heterogeneous nature of the final product is shown in Figure 2g.

An example of a rolled, relatively regular oligomeric nanotubular structure, made of a very thin nanosheet, is shown in Figure 3a.

Depending on how thick the nanosheets/nanoflakes are, different products result. Nanosheets with different thicknesses are shown in Figure 4. As we can see, the fairly thin one (thickness a few nanometers; Figure 4a) can freely roll and make a tubular morphology. As the thickness increases (20−100 nm), the curling gets more difficult (Figure 4b); finally, relatively thick and flat flakes are produced (Figure 4c).

The PANI nanotubes ("pH 2.5 20 h") obtained from the pH stat experiment at pH 2.5 are shown in Figure 5. To get more information about the morphology of the inner part of the nanotubes, we have crushed the product in a mortar

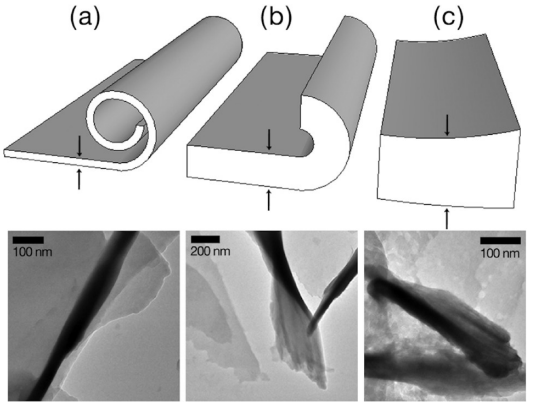

Figure 4. TEM micrographs of (a−c) the "falling pH 1 h" sample along with the corresponding schemes that illustrate different thicknesses.

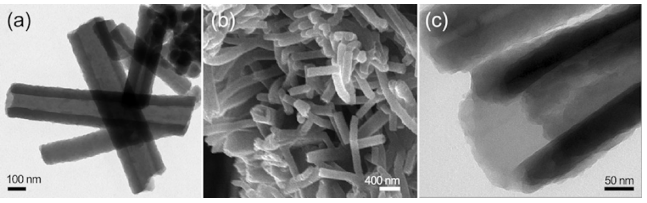

Figure 5. (a,c) TEM and (b) SEM micrographs of the "pH 2.5 20 h" sample.

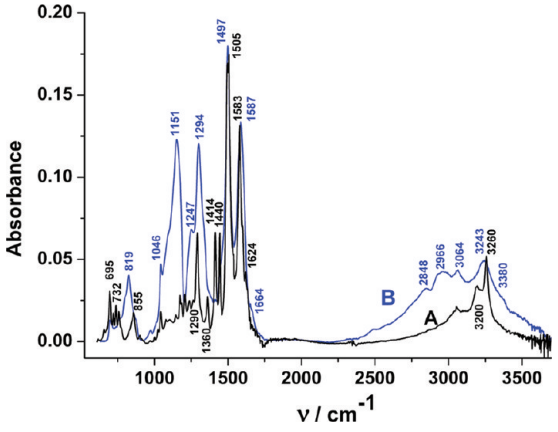

Figure 6. FTIR spectra of (A) the "falling pH 1 h" and (B) "pH 2.5 20 h" samples.

(Figure 5c). This Figure shows the inner part of a partially broken nanotube that looks fairly smooth (possibly oligomeric nanotube inner walls), whereas the outer walls are relatively coarse because of the irregular polyaniline polymer formed at lower pH.

The "pH 2.5 20 min" control experiment where the reaction was kept at pH 2.5 before the sample was quickly taken for TEM analysis confirmed the presence of nanosheets and curled nanostructures (Supporting Information).

FTIR. The FTIR spectra of the nanoflakes ("falling pH 1 h") and PANI nanotubes ("pH 2.5 20 h") samples are shown in Figure 6A,B. The region from around 3060 to 2900 cm^{-1} (Figure 6A,B) can be attributed to the vibrational mode of C−H bonds.[42] The bands at 3260 and 3200 cm^{-1} in the spectrum of the "falling pH 1 h" sample and the band at 3243 cm^{-1} in the nanotube spectrum can be assigned to N−H····N stretching vibrations of the secondary amine because of different types of intra- and intermolecular hydrogen bonds.[43]

The spectrum of the "falling pH 1 h" sample surprisingly does not exhibit bands of significant intenisity at ca. 3400 and 3380 cm^{-1} corresponding to the free N−H stretching vibration of primary ($-NH_2$) and secondary amine (−NH) groups.[22−24,43] In the spectrum of the "pH 2.5 20 h" sample this region is more pronounced indicating more stretching vibration modes from free N−H. Also, the C−H region (the C−H stretching bands from the aromatic rings are clearly visible at 3064, 2966, and 2848 cm^{-1}) has a higher intensity in the spectrum of the "pH 2.5 20 h" sample compared with the same region in the "falling pH 1 h" sample spectrum. The lack of the vibrational modes of C−H bonds in the "falling pH 1 h" sample spectrum confirms their highly cross-linked structure. Therefore, according to the aforementioned results and the clear presence of the bands at 3260 and 3200 cm^{-1} in the spectrum of the "falling pH 1 h" sample, we can conclude that there should be nitrogen sites in the initial structures that favor hydrogen bonding.

In addition, there are weak carbonyl bands at 1624 and 1664 cm^{-1} that could be assigned to a hydrogen-bonded C=O stretch, that is, —C=O· · · H−N−.[25] (This band has also been assigned to stretching vibrations of C−C bonds characteristic of both tri- and tetrasubstituted aromatic groups.[24,25]) These weak bands seen in the "falling pH 1 h" and "pH 2.5 20 h" spectra, overlapped by intense bands at 1583 and 1587 cm^{-1} and the bands at 1497 and 1505 cm^{-1}, can be attributed to C=C stretching in the quinoid and benzenoid rings, respectively. The bands at 1414 and 1444 cm^{-1} clearly visible in the "falling pH 1 h" sample spectrum could be assigned to branched phenazine-like structures. Indeed, these bands diminish in intensity (because of more para-coupling, less branching) as the reaction progresses and the pH decreases (the shoulder in the "pH 2.5 20 h" spectrum).[19,20] Low intensity bands at 1360 and 1174 cm^{-1} in the spectrum of the "falling pH 1 h" sample and the high intensity band at 1151 cm^{-1} in the "pH 2.5 20 h" sample are attributed to C=N stretching. For a regular polyaniline, strong bands appear at ca. 1160 cm^{-1} (sometimes referred to as an electronic band) and at ca. 1140 cm^{-1} (C−H in plane bending vibration).[44] It is interesting to note that the peak at 1294 cm^{-1} increases in intensity, and the peak at 1151 cm^{-1} in the "pH 2.5 20 h" spectrum is shifted toward higher wavenumbers and is much more intense compared with the peak at 1174 cm^{-1} seen in the "falling pH 1 h" sample spectrum. This (if we assign this band to a C−H in plane bending vibration) implies the increasing occurrence of linear structures. It has been suggested that the 1046 cm^{-1} band is characteristic of the S=O stretching vibration mode from the sulfate group.[23,24] This band is present in both samples. The bands at 695 and 735 cm^{-1} (the "falling pH 1 h" sample) are associated with out-of-plane C−C deformation vibrations and out of plane C−H bending, respectively, in monosubstituted aromatic rings.[45] Because monosubstituted rings are always terminal in the chain, the bands associated with them are clearly visible only in spectra of short-chain oligoanilines. As the chain length increases, their intensity continues to decrease, which is confirmed by their low intensity in the "pH 2.5 20 h" spectrum. Also, there is a band at 858 cm^{-1} that originates from the branched 1,2,4-trisubstituted ortho-coupled benzene rings. This band is still visible as a shoulder in the "pH 2.5 20 h" spectrum, but the main peak is now at 820 cm^{-1}, which should originate from C−H out-of-plane bending in 1,2-disubstituted ring structures (para-coupling), indicating that a head-to-tail coupling of aniline occurs during the polymerization at pH 2.5.

According to this FTIR data, the "falling pH 1 h" sample could partially consist of phenazine-like branched structures that are still visible in the "pH 2.5 20 h" structure, although the para-coupling clearly dominates during the formation of the nanotubes. It is well-known that electrochemical polymerization of 2-aminodiphenylamine (ortho-substituted aniline dimer) produces "flaky" structures (similar to the one shown in Figure 1A), whereas 4-aminodiphenylamine (para-substituted aniline dimer) creates more nanofiber- or nanorod-like structures.[46]

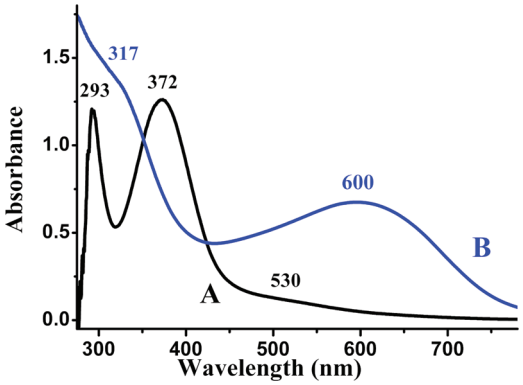

Figure 7. UV−vis spectra of (A) the "falling pH 1 h" and (B) the "pH 2.5 20 h" samples.

UV−vis. The emeraldine base form of polyaniline usually absorbs strongly in two areas, with maxima at 320−330 and 600−660 nm. The first band is assigned to $\pi-\pi^*$ excitation of the para-substituted benzenoid segment (−B−NH−B−NH), whereas the other is associated with the excitation of the quinoid segment (−N=Q=N−).[45]

The UV−vis spectrum of the "falling pH 1 h" sample (Figure 7A), has two strong $\pi-\pi^*$ peaks at 293 and at 372 nm and a weak $n-\pi^*$ shoulder at ∼530 nm. This is consistent with the previously proposed presence of substituted quinone (strong $\pi-\pi^*$ peak centered at 250−314 nm, a medium $\pi-\pi^*$ peak centered at 308−398 nm, and in some cases, a weak $n-\pi^*$ band centered at 424−525 nm).[25] The reason for the stronger $\pi-\pi^*$ peak at 372 nm in our spectrum could be the presence of the additional leucoemeraldine-type oligomer structures whose peak is superimposed on the peak from substituted quinones. These could be obtained because of the hydrolytic reactions at higher pH in the presence of a strong oxidizing agent. Finally, the lack of a peak at ca. 600 nm because of −N=Q=N−, which is usually part of the emeraldine base structure, could be due to the presence of O=Q=N− groups.[38] In this case, both O and N could be preferred sites for hydrogen bonding.

As the para coupling becomes more significant (Figure 7), a peak at 622 nm (from N=Q=N− quinoid units) appears in the spectrum of the "pH 2.5 20 h" sample. At the same time, the benzenoid region shows a broad shoulder, which implies overlapping of different peaks, one of which could be due to the presence of the peak at 293 nm and the other due to the peak at 372 nm. This is because the material is not pure polyaniline but a mixture of this with the oligomeric material that gives the spectrum in Figure 7A. The result is a broad shoulder of absorption due to overlapping of the bands as the two types of material were present. However, the UV−visible spectrum of the "pH 2.5 20 h" sample implies the increasing presence of typical polyaniline structural units.

XRD. The XRD pattern of the "falling pH 1 h" sample indicates partial crystallinity (Figure 8). The main diffraction peaks are at 2θ values of 6.4, 18.4, 23.1, 25.6, and 28.2°. The peaks are superimposed on a broad background, which suggests the presence of an amorphous phase. This XRD pattern is very similar to that reported in a paper on

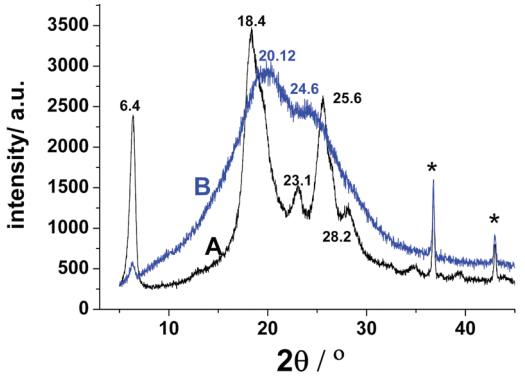

Figure 8. XRD pattern of (A) the "falling pH 1 h" and (B) the "pH 2.5 20 h" samples. The peaks denoted with asterisks are from a sample holder.

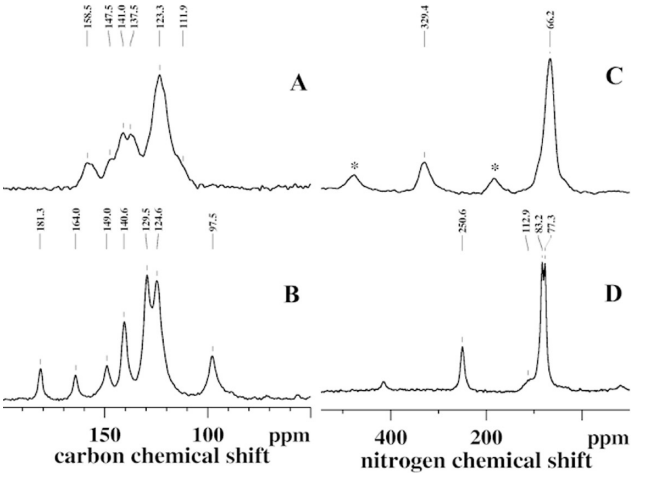

Figure 9. ^{13}C NMR spectra of (A) the standard polyaniline, (B) the "falling pH 1 h" sample, (C) ^{15}N spectra of standard polyaniline, and (D) the "falling pH 1 h" sample. The spinning sidebands are denoted by asterisks.

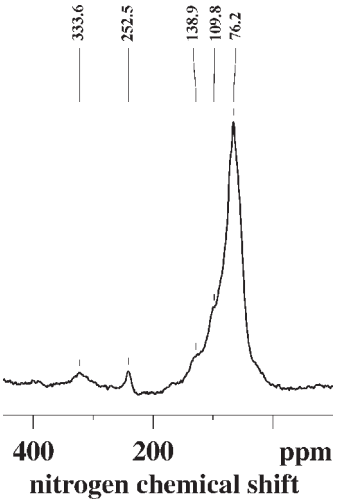

Figure 10. ^{15}N NMR spectrum of the "pH 2.5 20 h"sample.

hierarchical 3-D structures obtained for aniline oxidation products synthesized in strongly alkaline solutions.[47] This implies that there are similar reaction pathways or formation mechanisms for the reactions at high and medium pH (12.0 and 7.0, respectively). The peak at $2\theta = 6.4°$ (corresponding to a spacing of 13.8 Å, i.e., long-range order) was previously assigned to the periodicity caused by the aniline/dopant acid salt,[10] and it is only observed for highly ordered samples. It is believed that the polyaniline interplanar distance increased by the effective penetration of dopant molecules and that the peak at $2\theta = 6.4°$ arises from the formation of a lamella between the polyaniline chains.[48] Because we have not detected the presence of alanine, either in the ^{15}N spectra or the ^{13}C SSNMR spectra,[20] this peak could be assigned to the periodicity between chains and sulfate counterion. The presence of sulfate is confirmed by the FTIR peak at 1046 cm^{-1}. The peaks at 18.4 and 25.6° are usually assigned to the periodicity parallel and perpendicular to the polymer chain, respectively.[44] The peaks at 23.1 and 28.2° (corresponding to spacing of 3.1 and 3.8 Å) could be due to a periodicity caused by $\pi-\pi$ stacking of rigid phenazine-like structures.[39,40] Taken altogether, the observed peaks confirm the presence of short- and long-range order in the structure of the nanoflakes.

In the "pH 2.5 20 h" XRD pattern, the peak at $2\theta = 6.4°$ significantly decreases in intensity, indicating less ordering of nanotubes, which is also noticeable from the broad peaks at 20.1 and 24.6°. This could mean that although we could still have the presence of nanoflake structures (even in the pH stat experiment done at pH 2.5, see Figure 2g), the polymerization produces polyaniline with less-ordered structure, which simply polymerizes from or covers up the walls of the rolled nanosheets.

NMR Experiments. Figure 9 shows the solid-state ^{13}C and ^{15}N CPMAS NMR spectra of standard, chemically synthesized polyaniline[1,2,50] (in parts A and C of the Figure) and the spectra of the "falling pH 1 h" sample (parts B and D). There are clear differences between the spectra of polyaniline and the"falling pH 1 h" sample. The most obvious differences in the carbon spectrum are the presence of the new peaks at 181.3 and 97.5 ppm for "falling pH 1 h" sample (Figure 9B). This spectrum is similar (except for the peaks at 181.6 and 164.0 ppm) to the ^{13}C spectrum obtained from *poly*-(*ortho*-diphenylamine) (OPD) where phenazine-like units are expected.[41] The peaks at 181.3 and 164.0 ppm could originate from C═O and C═N carbons, not characteristic for *poly*-(*ortho*-diphenylamine).[41] This is in line with the FTIR and UV−vis results detailed in the previous sections and in our previous paper[20] and with the recent report of Kriz et al.,[49] who investigated products obtained in the early stages of the oxidative polymerization of aniline in solutions using ^{1}H, ^{13}C, and ^{15}N 1-D and 2-D NMR spectroscopy and ^{1}H PFG NMR.

The ^{15}N spectra of PANI and the "falling pH 1 h" sample are also different. The "standard" PANI spectrum shown in Figure 9C has peaks at 66.2 and 329.4 ppm, from amine and imine nitrogen atoms, respectively.[50a] However, the spectrum of the "falling pH 1 h" sample has different amine sites, with peaks at 77.3 and 83.2 ppm and a small shoulder at ~110 ppm. Also, there is a relatively narrow peak at 250.6 ppm, which is shifted upfield by ca. 70 ppm compared with that of the imine peak at 321.8 ppm in the PANI spectrum. The cross-relaxation time T_{NH} for the peak at 250.6 ppm is ~140 μs,[20] which implies a close proximity to hydrogen. The ^{15}N spectrum of the "pH 2.5 20 h" sample is shown in Figure 10. The broad, intense composite peak, which consists of at least three resonances (76.2, 109.8, and 138.9 ppm), dominates the spectrum. This implies a complex molecular structure with several different −NH groups. The peak at ca. 250 ppm is much less intense compared with the same peak in the spectrum of the "falling pH 1 h" sample. However, its presence could be another indication of the occurrence of nanoflakes in the final PANI nanotube

Scheme 1

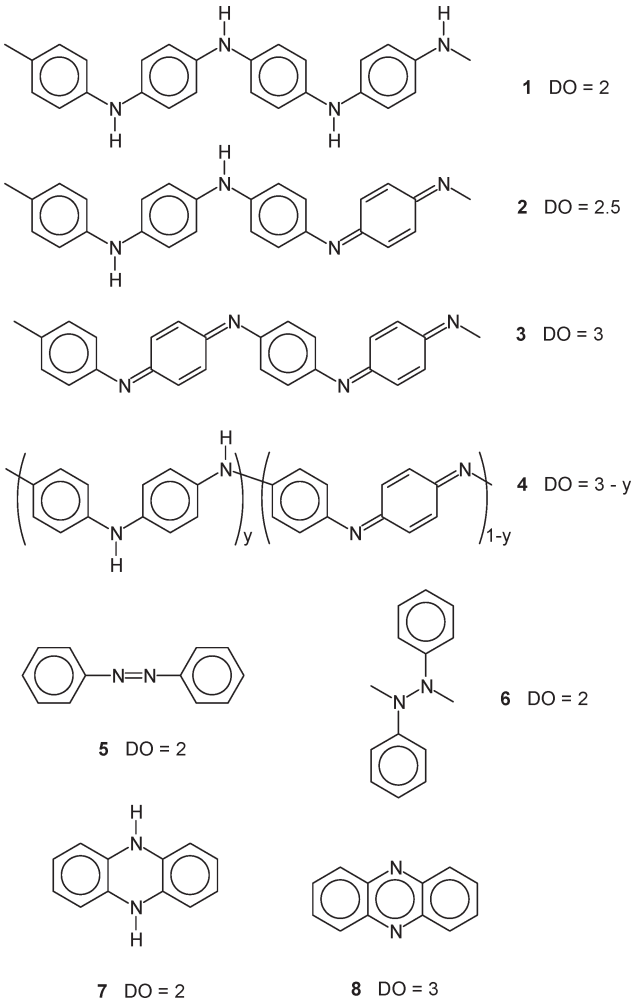

Scheme 2

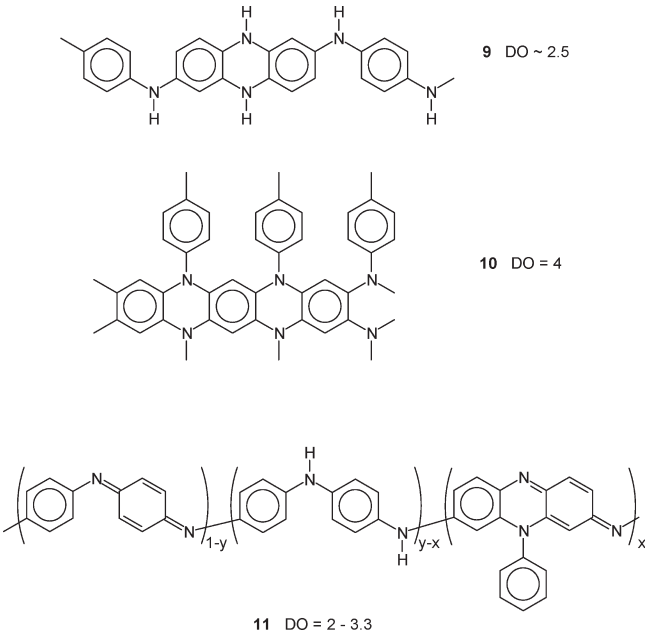

Scheme 3

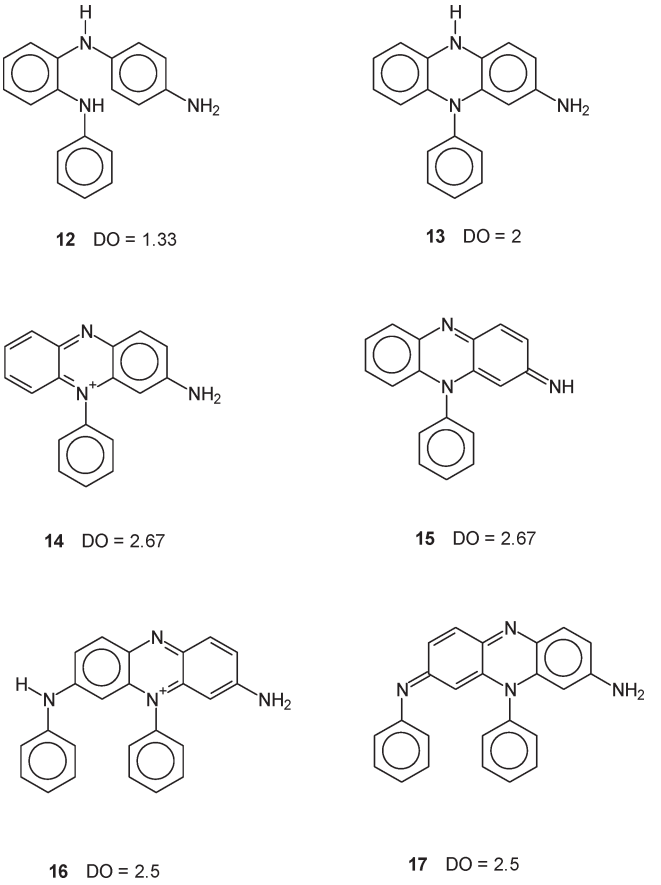

structure obtained at a relatively low pH of 2.5. (See Figure 2g.) The additional characteristic feature is the peak at ~330 ppm that originates from imine structures, as seen in the standard PANI spectrum, Figure 9C. This is in line with the UV−vis data and the presence of the peak at 600 nm in the PANI nanotube spectrum. Therefore, the PANI nanotube formation in a later stage includes a greater proportion of para-coupled units compared with the structures initially formed.

Molecular Structure. An important aspect of the structure of 2-D nanosheets is the chemical nature of the aniline oxidation products that are formed under various conditions. Some of the molecular structures that have been proposed for such products are shown in Schemes 1−3. One of the aims of this work is to determine which of these structures are the most feasible based on the data obtained through the application of different techniques.

At low pH, the standard polyaniline structures leucoemeraldine base **1**, emeraldine base **2**, pernigraniline **3**, or an intermediate form **4** (or protonated forms thereof) are obtained with a degree of oxidation (DO; defined as the number of electrons removed per aniline monomer unit in the oxidation) in the range of 2 to 3. Under the normal conditions of reaction using persulfate as the oxidant, the product is close in composition to the emeraldine salt form of **2**, with DO = 2.5. The situation for reactions carried out at high initial pH is rather more complex and uncertain. The formation of diazine **5** or polyazane **6** structures can occur with DO = 2, and it has been proposed that the material obtained as microspheres from the persulfate oxidation of aniline in dilute (0.01 M) solution in the absence of initially added acid contains polyazane structures.[25] For similar reactions carried out at higher concentrations (0.1 M), the presence of "phenazine-like" structures has been postulated.[23] The formation of phenazine **8** from aniline involves

ortho rather than para coupling of the aniline units and requires a relatively high degree of oxidation, DO = 3. Such a reaction has been reported but only under rather extreme experimental conditions involving the use of supercritical water.[51] The formation of dihydrophenazine **7** from aniline involves a lower degree of oxidation, DO = 2, which is more comparable to the values involved in the formation of polyaniline.

There have been several reports postulating the formation of phenazine units within polymeric structures formed by oxidative coupling of polyaniline, and some of these are shown in Scheme 2. Structure **9** involves the incorporation of a dihydrophenazine unit within a polyaniline chain and has been postulated to be a product of the electrochemical polymerization of aniline.[52] However, the incorporation of the dihydrophenazine unit in the structure in this way cannot be achieved without the addition of an extra NH group, so this is not a true polymer of aniline (i.e., the C/N ratio is not 6). An alternative way of incorporating phenazine-like units in a polymer derived from aniline is shown in **10**, a 2-D polymer, which has been postulated to be a product of the electrochemical polymerization of aniline.[53] The degree of oxidation of aniline required to form this polymer, DO = 4, is very high, and the study that resulted in this proposed material was carried out electrochemically under extreme conditions involving the use of anhydrous HF. Structure **11** containing phenazine-like units has recently been proposed for polyaniline prepared under normal aqueous solvent conditions.[54] The structure of the phenazine-like unit involved is intermediate between those of dihydrophenazine **7** and phenazine **8** and is referred to as an "*N*-phenylphenazine" stuctural unit.[55]

The formation of oligomers involving *N*-phenylphenazine stuctural units is illustrated in Scheme 3. These result from both ortho and para coupling of aniline molecules as in **12**, which can form *N*-phenylphenazine stuctural units **13** and **14** upon further oxidation. A further meta/para coupling results in the formation of "pseudomauvine", shown in Scheme 3 in the salt form **16** or the base form **17**.[54,55] The base form of **14** is **15**,[56] and this is the parent of the *N*-phenylphenazine unit that is incorporated in the polymeric structure **11**.[54]

Many proposals have been presented for the molecular structure of the materials produced by the oxidation of aniline, some of which are shown in Schemes 1−3.[23,25,52−54] Even for reactions carried out under similar experimental conditions, the existence of such a range of possibilities might suggest that a range of different molecular species might be present either in the product of a single reaction or when comparing products of reactions carried out under slightly different conditions. However, the results of the present and our previous studies of aqueous solution syntheses[19,20,32] have shown that there are essentially just two types of product, the one observed in "falling pH 1 h" sample in the present study, which is formed at pH > 5, and the emeraldine form of polyaniline, which is formed at pH < 3. The product obtained at intermediate pH is a mixture of these two forms.[30] Inspection of the FT-IR spectra in a recently reported study of the persulfate oxidation of aniline in methanol solution in the absence of initially added acid[57] shows that this is the case for this system as well. However, in this article, the self-curling effect in forming oligomeric nanotubes is attributed to the presence of methanol. According to Huang and Lin,[57] the nanosheets are accompanied by irregular aggregates that were observed when no methanol was added to the solution. They stated that the protonation of para-coupling PANI provides the main driving force that causes PANI intermediates to transform into PANI nanotubes through a self-curling process. However, we have shown that early formed nanosheets do accompany irregular morphologies and also form oligomeric nanotubes that roll, probably tending to decrease the surface energy.

The very simple ^{15}N NMR spectrum of the high-pH product, exemplified by that of the "falling pH 1 h" sample in Figure 9D, eliminates many of the previously proposed molecular structures shown in Schemes 2 and 3. For example, structure **10** has no amine N atoms and would only give a single ^{15}N NMR signal. Structure **11** would contain signals due to the emeraldine form of polyaniline, as in Figure 9C, and two further imine nitrogen signals from the *N*-phenylphenazine" part of the structure. Similar criticisms apply to the oligomeric structures **14**, **16**, and **17** in Scheme 3, which contain more than one imine nitrogen atom, in contradiction to the observed spectrum. This is also true of the *N*-phenylphenazine molecule **15**, but if further oxidation occurs as in **18** or in a corresponding oligomeric form, then reasonable agreement with the

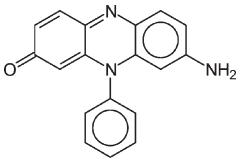

18

observed spectra is obtained. In particular, this agrees with the presence of a carbonyl carbon signal in the ^{13}C CP MAS NMR (181.3 ppm; see above and Zujovic et al.[20]) and in the high-resolution spectra of aniline oligomers reported recently.[49] However, there is still a question of whether the peak at ca. 250 ppm could be assigned to uncharged imine nitrogens, hydrogen bonded with a proton from the amine nitrogens that give rise to the signals at ca. 80 ppm.[20] Whereas there is insufficient evidence to prove unambiguously the molecular structure of the high-pH product, this analysis shows how the spectroscopic results can be used to eliminate many of the previously proposed molecular structures and should help to focus any future discussions or hypotheses on the nature of the material concerned.

Conclusions

In summary, the phenomenon of nanosheet rolling and its implications for the genesis of self-assembled polyaniline nanotubes is reported and confirmed through SEM and TEM. We showed that there are basically two stages during the formation of PANI nanotubes: (a) The first stage is curling or rolling of nanosheets and the formation of smooth oligomeric nanotubes. These are probably formed in the first stage of oxidative polymerization from oligomers when the pH did not reach a constant 2.5 value in the pH-stat experiment. (b) The second stage is polyaniline polymerization when these oligomeric nanotubes serve in a later stage as templates for the formation of PANI nanotubes at lower pH. The 1 h product that was obtained at a pH of ~3.5 consisted of relatively ordered oligomeric structures (stacked nanosheets) exhibiting the ortho and para coupling of aniline monomers. The presence of hydrogen bonds is suggested on the basis of FTIR and is consistent with XRD results. The presence of $\pi-\pi$ stacking has also been proposed on the basis of XRD experiments. These interactions are likely to drive the assembly of basic units (i.e., short oligomers, neutral aniline molecules, and anilinium cations) toward intermediate 2-D nanosheets and finally onto 3-D nanotube structures at lower

pH. There are some questions that should be answered and corresponding experiments that should be carried out. The pH, the temperature, and the concentration should be correlated to different initial structures taken from dilute solutions and detailed structural investigations of these structures should be performed. The interactions that drive the formation of these initial supramolecular structures should be further explored. According to previously extensively published material, the formation mechanisms and the genesis of various products during the oxidative aniline polymerization is a quite complex problem,[20−25,28−31] and the corresponding experiments regarding these are being carried out in our laboratories.

Acknowledgment. We gratefully acknowledge the New Zealand Foundation for Science and Technology for financial support for this work (New Economy Research Fund, contract no. UOAX0408) and the EPSRC (U.K.). We thank Dr. Lijuan Zhang for stimulating discussions and comments and Dr. Geoff Waterhouse for high-quality TEM micrographs and useful comments.

Supporting Information Available: TEM micrographs of the "pH 2.5 20 min" sample, which is obtained in the control experiment. This material is available free of charge via the Internet at http://pubs.acs.org.

References and Notes

(1) Heeger, A. J. *Synth. Met*. **2002**, *125*, 23.
(2) Trivedi, D. C. In *Handbook of Organic Conductive Molecule and Polymers*, Naiwa, H. S., Ed.; Wiley: Chichester, U.K., 1997; Vol. *2*, pp 505−72 and references therein.
(3) Choi, S.; Park, S. *Adv. Mater*. **2000**, *12*, 1547.
(4) Huang, J.; Virji, S.; Weiller, B. H.; Kaner, R. B. *J. Am. Chem. Soc*. **2003**, *125*, 314.
(5) Ramanathan, K.; Bangar, M. A.; Yun, M.; Chen, W.; Myung, N. V.; Mulchandani, A. *J. Am. Chem. Soc*. **2005**, *127*, 496.
(6) Zhang, L.; Peng, H.; Zujovic, Z. D.; Kilmartin, P. A.; Sejdic, J. T. *Macromol. Chem. Phys*. **2007**, *208*, 1210–1217.
(7) Zhang, L.; Wan, M.; Wei, Y. *Macromol. Rapid Commun*. **2006**, *27*, 366–371.
(8) Zhang, L.; Wan, M.; Wei, Y. *Synth. Met*. **2005**, *151*, 1–5.
(9) Zhang, L.; Wan, M. *Thin Solid Films* **2005**, *477*, 24–31.
(10) Zhang, L.; Long, Y.; Wan, M.; Chen, Z. *Adv. Funct. Mater*. **2004**, *14*, 693–698.
(11) Zhang, L.; Wan, M. *Adv. Funct. Mater*. **2003**, *13*, 815–820.
(12) Zhang, L.; Wan, M. *J. Phys. Chem. B* **2003**, *107*, 6748–6753.
(13) Zhang, L.; Wan, M. *Nanotechnology* **2002**, *13*, 750–755.
(14) Huang, J.; Kaner, R. B. *J. Am. Chem. Soc*. **2004**, *126*, 851–855.
(15) Virji, S.; Huang, J.; Kaner, R. B.; Weiller, B. H. *NanoLett*. **2004**, *4*, 491.
(16) Huang, J.; Virji, S.; Weiller, B. H.; Kaner, R. B. *Chem.—Eur. J*. **2004**, *10*, 1314.
(17) Tran, D. H; Kaner, R. B. *Chem Commun*. **2006**, 3915.
(18) Huang, J.; Kaner, R. B. *Angew. Chem., Int. Ed*. **2004**, *43*, 5817–5821.
(19) Zhang, L.; Zujovic, Z. D.; Peng, H.; Bowmaker, G. A.; Kilmartin, P. A.; Travas-Sejdic, J. *Macromolecules* **2008**, *41*, 8877–8884.
(20) Zujovic, Z. D.; Zhang, L.; Bowmaker, G. A.; Kilmartin, P. A.; Travas-Sejdic, J. *Macromolecules* **2008**, *41*, 3125–3135.
(21) Hopkins, A. R.; Lipeles, R. A.; Hwang, S. *Synth. Met*. **2008**, *158*, 594–601.
(22) Stejskal, J.; Sapurina, I.; Trchova, M.; Konyushenko, E. N.; Holler, P. *Polymer* **2006**, *47*, 8253–8262.
(23) Trchova, M.; Sedenkova, I.; Konyushenko, E. N.; Stejskal, J.; Holler, P.; Ciric-Marjanovic, G. *J. Phys. Chem. B* **2006**, *110*, 9461–9468.
(24) Konyushenko, E. N.; Stejskal, J.; Sedenkova, I.; Trchova, M.; Sapurina, I.; Cieslar, M.; Prokes, J. *Polym. Int*. **2006**, *55*, 31–39.
(25) Venancio, E. C.; Wang, P.-C.; MacDiarmid, A. G. *Synth. Met*. **2006**, *156*, 357–369.
(26) Pinto, N. J.; Johnson, A. T.; MacDiarmid, A. G.; Mueller, C. H.; Theofylaktos, N.; Robinson, D. C.; Miranda, F. A. *Appl. Phys. Lett*. **2003**, *83*, 4244–4246.
(27) Wang, C.; Wang, Z.; Li, M.; Li, H. *Chem. Phys. Lett*. **2001**, *341*, 431–434.
(28) Wu, J.; Tang, Q.; Li, Q.; Lin, J. *Polymer* **2008**, *49*, 5262–5267.
(29) Song, S.; Pan, L.; Li, Y.; Shio, Y.; Pu, L.; Zhang, R.; Zheng, Y. *Chin. J. Chem. Phys*. **2008**, *2*, 21.
(30) Wei, Z.; Zhang, Z.; Wan, M. *Langmuir* **2002**, *18*, 917–921.
(31) Ding, H.; Shen, J.; Wan, M.; Chen, C. *Macromol. Chem. Phys*. **2008**, *209*, 864–871.
(32) Laslau, C.; Zujovic, Z. D.; Zhang, L.; Bowmaker, G. A.; Travas-Sejdic, J. *Chem. Mater*. **2009**, *21*, 954–962.
(33) Geng, B.; Zhan, F.; Jiang, H; Guo, Y.; Xing, Z. *Chem. Commun*. **2008**, 5773–5775 and references therein .
(34) Laslau, C.; Zujovic, D.; Travas-Sejdic, J. *Macromol. Rapid Commun*. **2009**, *30*, 000–000.
(35) Stejskal, J.; Sapurina, I. *J. Colloid Interface Sci*. **2004**, *274*, 489–495.
(36) MacDiarmid, A. G.; Epstein, A. J. *Faraday Discuss. Chem. Soc*. **1989**, *88*, 317–332.
(37) (a) Hayashi, S.; Hayamizu, K. *Bull. Chem. Soc. Jpn*. **1991**, *64*, 688–691. (b) Martin, G. E.; Hadden, C. E. *J. Nat. Prod*. **2000**, *63*, 543–585.
(38) Fu, Y.; Elsenbaumer, R. *Chem. Mater*. **1994**, *6*, 671.
(39) Gawlicka-Chruszcz, A.; Stadnicka, K. *Acta Crystallogr*. **2002**, *C58*, 0416–0420.
(40) Thalladi, V. R.; Smolka, T.; Boese, R.; Sustmann, R. *CrystEngComm* **2000**, 17.
(41) Sun, X.; Dong, S.; Wang, E. *Macromol. Rapid Commun*. **2005**, *26*, 1504.
(42) Angelopoulos, M.; Dipietro, R.; Zheng, W. G.; MacDiarmid, A. G.; Epstein, A. J. *Synth. Met*. **1997**, *84*, 35.
(43) Zheng, W.; Angelopoulos, M.; Epstein, A. J.; MacDiarmid, A. G. *Macromolecules* **1997**, *30*, 2953.
(44) Jin, E.; Liu, N.; Lu, X.; Zhang, W. *Chem. Lett*. **2007**, *36*, 1288–1289.
(45) Laska, J.; Widlarz, J. *Polymer* **2005**, *46*, 1485.
(46) Cotarelo, M. A.; Huerta, F.; Quijada, C.; Mallavia, R.; Vazquez, J. L. *J. Electrochem. Soc*. **2006**, *153*, D114–D122.
(47) Zhou, C.; Han, J.; Song, G.; Guo, R. *Eur. Polym. J*. **2008**, *44*, 2850–2858.
(48) Jana, T.; Chatterjee, J.; Nandi, A. K. *Langmuir* **2002**, *18*, 5720.
(49) Kriz, J.; Starovoytova, L.; Trchova, M.; Konyushenko, E. N.; Stejskal, J. *J. Phys. Chem B* **2009**, *113*, 6666–6673.
(50) (a) Zujovic, Z. D.; Gizdavic-Nikolaidis, M.; Kilmartin, P. A.; Idriss, H.; Senanayake, S. D.; Bowmaker, G. A. *Polymer* **2006**, *47*, 1166. (b) Zujovic, Z.; Gizdavic-Nikolaidis, M.; Kilmartin, P. A.; Travas-Sejdic, J.; Cooney, R. P.; Bowmaker, G. A. *Appl. Magn. Reson*. **2005**, *28*, 123.
(51) Ding, J. *Huagong Xuebao* **2000**, *51*, 690–694.
(52) Bartlett, P. N.; Birkin, P. R.; Palmisano, F.; Benedetto, G. D. *J. Chem. Soc., Faraday Trans*. **1996**, *92*, 3123–3130.
(53) Genies, E. M.; Lapkowski, M.; Penneau, J. F. *J. Electroanal. Chem*. **1988**, *249*, 97–107.
(54) Ciric-Marjanovic, G.; Konyushenko, E. N.; Trchova, M.; Stejskal, J. *Synth. Met*. **2008**, *158*, 200–211.
(55) Ciric-Marjanovic, G; Trchova, M.; Stejskal, J. *Int. J. Quantum Chem*. **2008**, *108*, 318–333.
(56) Sapurina, I.; Stejskal, J. *Polym. Int*. **2008**, *57*, 1295–1325.
(57) Huang, Y. F.; Lin, C. W. *Polymer* **2009**, *50*, 775–782.